Electrochemical Studies on Metal Derivatives of Buckminsterfullerene (C_{60})

Susan A. Lerke,[†] B. A. Parkinson,[‡,§] Dennis H. Evans,*[,†] and Paul J. Fagan*[,‡]

Contribution from the Department of Chemistry and Biochemistry, University of Delaware, Newark, Delaware 19716, and Contribution No. 6173 from the Central Research and Development Department, E. I. du Pont de Nemours and Co., Inc., Experimental Station, P.O. Box 80328, Wilmington, Delaware 19880-0328. *Received February 14, 1992*

Abstract: The electrochemical properties of the complexes $(Ph_3P)_2Pt(\eta^2\text{-}C_{60})$, $(Et_3P)_2M(\eta^2\text{-}C_{60})$, $[(Et_3P)_2M]_6C_{60}$ (M = Ni, Pd, Pt; Et = ethyl, Ph = phenyl), and $[(Et_3P)_2Pt]_nC_{60}$ (n = 2-4) have been investigated. In the case of the monosubstituted complexes $(Ph_3P)_2Pt(\eta^2\text{-}C_{60})$ and $(Et_3P)_2M(\eta^2\text{-}C_{60})$, three to four sequential one-electron reduction waves are observed shifted to more negative potentials relative to C_{60}. Reduction is accompanied by loss of the metal fragment $(R_3P)_2M$. The rate of metal dissociation upon reduction is dependent on the identity of the phosphine ligand ($(Ph_3P)_2Pt(\eta^2\text{-}C_{60})^{2-} > (Et_3P)_2Pt(\eta^2\text{-}C_{60})^{2-}$), the metal (Ni > Pd > Pt), and the extent of reduction ($(Et_3P)_2PtC_{60}^{3-} > (Et_3P)_2PtC_{60}^{2-} > (Et_3P)_2PtC_{60}^{-}$). The cyclic voltammograms have been simulated to obtain kinetic and thermodynamic information regarding these processes. The reduction events in the metal complexes are C_{60}-centered, whereas the irreversible oxidation waves observed for these complexes are proposed to be metal-centered from comparison with the model complexes $(Et_3P)_2M(\eta^2\text{-}CH_2{=}CHCO_2CH_3)$ (M = Ni, Pd, Pt). The results lead to the conclusion that there is negligible extension of d-orbital backbonding density beyond the carbon-carbon double bond where the metal is attached. Coordination of one of these metals to C_{60} is proposed to lower the electron affinity of the carbon cluster by effectively removing one of the C_{60} carbon-carbon double bonds from conjugation and inductively adding electron density to the σ bond framework. Addition of more metals continues to lower the electron affinity of the C_{60} core, with the reversible potentials for $[(Et_3P)_2Pt]_nC_{60}$ shifting 0.36 V in the negative direction with each metal added for n = 0-4.

Introduction

We have been interested in the effect of metal coordination on the properties of buckminsterfullerene (C_{60}).[1] The electrochemistry of C_{60} itself has now been studied extensively,[1h,2] and up to five reduction waves have been seen for C_{60} in solution.[2b] The existence of the solid state phase K_6C_{60} suggests that six electrons can be accommodated on the C_{60} sphere.[3] Little is known about the electrochemical properties of C_{60} derivatives where the structure has been definitively established, although some preliminary data have appeared for the products of addition of diphenylcarbene[4] and for the iridium complex $(\eta^5$-indenyl)-$(CO)Ir(\eta^2\text{-}C_{60})$.[5] We have shown that the carbon-carbon double bonds in C_{60} behave chemically like electron-poor, strained alkenes (or arenes) and are reactive toward electron-rich metal reagents.[6] Metal coordination is expected to transfer electron density onto the C_{60} framework, but to what extent and how this is communicated across the sphere is not known. It has been found that the reactions of metal reagents can be quite selective, forming only monosubstituted metal derivatives in high yield rather than a mixture of multiply-substituted derivatives.[6] This selectivity can be explained if one assumes the coordination of one metal on C_{60} inhibits coordination of a second metal, i.e. decreases the electron affinity of the C_{60} sphere. Electrochemical studies would help address these points.

Here we report the electrochemical properties of the complexes $(Ph_3P)_2Pt(\eta^2\text{-}C_{60})$, $(Et_3P)_2M(\eta^2\text{-}C_{60})$, $[(Et_3P)_2M]_6C_{60}$ (M = Ni, Pd, Pt; Et = ethyl, Ph = phenyl), and $[(Et_3P)_2Pt]_nC_{60}$ (n = 2-4).[6] As we have shown elsewhere, the monosubstituted and hexasubstituted compounds have the structures **A** and **B**, respectively.[6] It is found that coordination of one metal shifts the reduction potentials of the C_{60} fragment to more negative potentials. The electron affinity decreases linearly with the sequential addition of each metal fragment. Addition of electrons to these metal-C_{60} complexes causes dissociation of the $(R_3P)_2M$ units. It is concluded that the major effect of dihapto metal coordination to C_{60} is to decouple electronically carbon-carbon double bonds from conjugation with those remaining uncoordinated and to donate inductively electron density to the σ bond framework, thereby lowering the electron affinity of the sphere. The results also show that backdonation of filled metal d-orbital electron density is primarily localized in the π^* orbital of the carbon-carbon double bond to which it is attached and does not extend significantly into

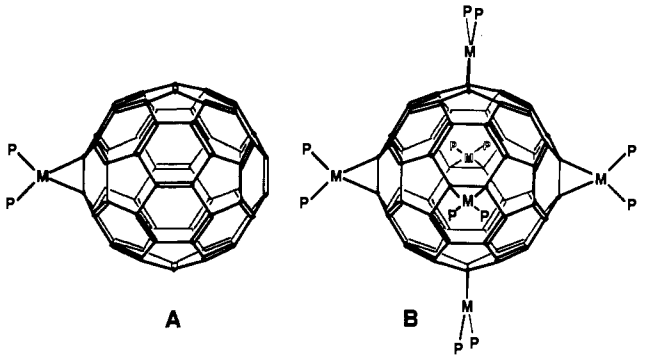

[†] University of Delaware.
[‡] E. I. du Pont de Nemours and Co., Inc.
[§] Present address: Chemistry Department, Colorado State University.

(1) (a) Krätschmer, W.; Lamb, L. D.; Fostiropoulos, K.; Huffman, D. R. *Nature* **1990**, *347*, 354-358. (b) Taylor, R.; Hare, J. P.; Abdul-Sada, A. K.; Kroto, H. W. *J. Chem. Soc., Chem. Commun.* **1990**, 1423-1425. (c) Kroto, H. W.; Heath, J. R.; O'Brien, S. C.; Curl, R. F.; Smalley, R. E. *Nature* **1985**, *318*, 162-163. (d) Stoddart, F. J. *Angew. Chem.* **1991**, *103*, 71. (e) Kroto, H. *Pure Appl. Chem.* **1990**, *62*, 407-415. (f) Kroto, H. *Science* **1988**, *242*, 1139-1145. (g) Hare, J. P.; Kroto, H. W.; Taylor, R. *Chem. Phys. Lett.* **1991**, *177*, 394. (h) Cox, D. M.; Behal, S.; Disko, M.; Gorun, S. M.; Greaney, M.; Hsu, C. S.; Kollin, E. B.; Millar, J.; Robbins, J.; Robbins, W.; Sherwood, R. D.; Tindall, P. *J. Am. Chem. Soc.* **1991**, *113*, 2940-2944. (i) Diederich, F.; Whetten, R. L. *Angew. Chem., Int. Ed. Engl.* **1991**, *30*, 678. (j) Miller, J. S. *Adv. Mater.* **1991**, *3*, 262. (k) Bethune, D. S.; Meijer, G.; Tang, W. C.; Rosen, H. J. *Chem. Phys. Lett.* **1990**, *174*, 219-222. (l) Ajie, H.; Alvarez, M. M.; Anz, S. J.; Beck, R. D.; Diederich, F.; Fostiropoulos, K.; Huffman, D. R.; Krätschmer, W.; Rubin, Y.; Schriver, K. E.; Sensharma, D.; Whetten, R. L. *J. Phys. Chem.* **1990**, *94*, 8630-8633. (m) Kroto, H. W.; Allaf, A. W.; Balm, S. P. *Chem. Rev.* **1991**, *91*, 1213-1235. (n) Krätschmer, W.; Fostiropoulos, K.; Huffman, D. R. *Chem. Phys. Lett.* **1990**, *170*, 167-180. (o) Curl, R. F.; Smalley, R. E. *Sci. Am.* **1991**, *265*, 54-63. (p) Smalley, R. E. *Acc. Chem. Res.* **1992**, *25*, 98-105. (q) Kroto, H. W. *Acc. Chem. Res.* **1992**, *25*, 106-112.

(2) (a) Haufler, R. E.; Conceicao, J.; Chibante, L. P. F.; Chai, Y.; Byrne, N. E.; Flanagan, S.; Haley, M. M.; O'Brian, S. C.; Pan, C.; Xiao, Z.; Billups, W. E.; Ciufolini, M. A.; Hauge, R. H.; Margrave, J. L.; Wilson, L. J.; Curl, R. F.; Smalley, R. E. *J. Phys. Chem.* **1990**, *94*, 8634-8636. (b) Dubois, D.; Kadish, K. M.; Flanagan, S.; Wilson, L. J. *J. Am. Chem. Soc.* **1991**, *113*, 7773-7774. (c) Allemand, P.-M.; Koch, A.; Wudl, F.; Rubin, Y.; Diederich, F.; Alvarez, M. M.; Anz, S. J.; Whetten, R. L. *J. Am. Chem. Soc.* **1991**, *113*, 1050-1051. (d) Dubois, D.; Kadish, K. M.; Flanagan, S.; Haufler, R. E.; Chibante, L. P. F.; Wilson, L. J. *J. Am. Chem. Soc.* **1991**, *113*, 4364-4366. (e) Jehoulet, C.; Bard, A. J.; Wudl, F. *J. Am. Chem. Soc.* **1991**, *113*, 5456-5457. (f) Kadish, K. M. Personal communication.

0002-7863/92/1514-7807$03.00/0

the π^* orbitals of the remaining double bonds. These observations help rationalize some of the chemical aspects of these metal-substituted C_{60} derivatives.

Experimental Section

The synthesis of the metal complexes $(Ph_3P)_2Pt(\eta^2\text{-}C_{60})$, $(Et_3P)_2M(\eta^2\text{-}C_{60})$, $[(Et_3P)_2M]_6C_{60}$ (M = Ni, Pd, Pt; Et = ethyl, Ph = phenyl), and $[(Et_3P)_2Pt]_nC_{60}$ (n = 2–4) used in this study is described elsewhere.[6] The complex $[(Et_3P)_2Pt]_2C_{60}$ exists as a mixture of three structural isomers. Similarly, for n = 3 and 4, each complex exists as a mixture of isomers with regard to the positions of the metal fragments on the C_{60} cluster.[6]

The complexes $(Et_3P)_2M(\eta^2\text{-}CH_2{=}CHCO_2CH_3)$ (M = Ni, Pd, Pt) were synthesized by reacting 1 equiv of freshly distilled, deoxygenated, and dried methyl acrylate with 1 equiv of the metal reagents $(Et_3P)_4M$[7] in dry deoxygenated toluene solution under nitrogen. After removal of solvent in high vacuum (10^{-4}–10^{-5} Torr), dry deoxygenated hexane was added to the residue, and this was filtered. Hexane was removed in vacuo to leave colorless to pale yellow oils. The platinum complex could be further purified by crystallization from a minimum of hexane at −78 °C with some difficulty encountered in initiating crystallization. Decantation of the supernatant yields a white solid which melts upon warming to room temperature. This complex is >95% pure by spectroscopic analysis. Because of the oily nature of the nickel and palladium products, and their refusal to crystallize at low temperatures from hexane, no further purification was attempted. Spectroscopic analysis reveals these oils to be the expected products which were ca. 92–95% pure. The complexes were air sensitive, but they appeared to be thermally stable for days when stored at −35 °C.

$(Et_3P)_2Ni(\eta^2\text{-}CH_2{=}CHCO_2CH_3)$: ^{1}H NMR (300 MHz, 25 °C, C_6D_6) δ 0.92 (overlapping quintets, 18 H, PCH_2CH_3), 1.33 (quintet, 6 H, PCH_2CH_3), 1.48 (quintet, 6 H, PCH_2CH_3), 1.88 (multiplet, 1 H, $CHH{=}CHCO_2CH_3$), 2.34 (multiplet, 1 H, $CHH{=}CHCO_2CH_3$), 3.27 (multiplet, 1 H, $CH_2{=}CHCO_2CH_3$), 3.55 (s, 3 H, $CH_2{=}CHCO_2CH_3$). ^{31}P NMR (121 MHz, 25 °C, C_6D_6) δ 23.3 (doublet, 1 P, $J_{P\text{-}P}$ = 33 Hz), 17.2 (doublet, 1 P, $J_{P\text{-}P}$ = 33 Hz).

$(Et_3P)_2Pd(\eta^2\text{-}CH_2{=}CHCO_2CH_3)$: ^{1}H NMR (300 MHz, 25 °C, C_6D_6) δ 0.95 (overlapping multiplets, 18 H, PCH_2CH_3), 1.35 (multiplet, 6 H, PCH_2CH_3), 1.50 (quintet, 6 H, PCH_2CH_3), 2.69 (multiplet, 1 H, $CHH{=}CHCO_2CH_3$), 3.27 (multiplet, 1 H, $CHH{=}CHCO_2CH_3$), 3.97 (multiplet, 1 H, $CH_2{=}CHCO_2CH_3$), 3.56 (s, 3 H, $CH_2{=}CHCO_2CH_3$). ^{31}P NMR (121 MHz, 25 °C, C_6D_6) δ 11.9 (doublet, 1 P, $J_{P\text{-}P}$ = 19 Hz), 16.8 (doublet, 1 P, $J_{P\text{-}P}$ = 19 Hz).

$(Et_3P)_2Pt(\eta^2\text{-}CH_2{=}CHCO_2CH_3)$: ^{1}H NMR (300 MHz, 25 °C, C_6D_6) δ 0.90 (overlapping multiplets, 18 H, PCH_2CH_3), 1.50 (multiplet, 6 H, PCH_2CH_3), 1.64 (multiplet, 6 H, PCH_2CH_3), 2.15 (multiplet, 1 H, $CHH{=}CHCO_2CH_3$, ^{195}Pt satellites, J^2_{PtH} = 44 Hz), 2.62 (multiplet, 1 H, $CHH{=}CHCO_2CH_3$, ^{195}Pt satellites, J^2_{PtH} = 48 Hz), 3.32 (multiplet, 1 H, $CH_2{=}CHCO_2CH_3$, ^{195}Pt satellites, J^2_{PtH} = 60 Hz), 3.57 (s, 3 H, $CH_2{=}CHCO_2CH_3$). ^{31}P NMR (121 MHz, 25 °C, C_6D_6) AB quartet centered at δ 17.8; simulation gives δ 17.2 and 18.4 with $J_{P\text{-}P}$ = 42 Hz; satellites owing to coupling to ^{195}Pt (33.8% abundance) give an ABX spectral pattern which was not simulated.

The C_{60} compounds were stored at −35 °C in a drybox. Ferrocene (Aldrich) was used as received. Tetrahydrofuran (Fisher) was purified by distillation from CaH_2 followed by distillation over Na/K alloy before being taken into the drybox. Dichloromethane (Fisher) was dried over molecular sieves (Mallinckrodt, 4 Å), distilled from calcium hydride, and degassed before being taken into the drybox. Tetra-*n*-butylammonium hexafluorophosphate ($TBAPF_6$) was obtained from Aldrich, recrystallized three times from ethanol, and vacuum dried at 85 °C for at least 18 h. Tetra-*n*-butylammonium perchlorate (TBAP) was obtained from Southwestern Analytical Chemicals, recrystallized two times from ethyl acetate, and vacuum dried overnight at 60 °C. In all cases, the concentration of electrolyte was 0.20 M. The electrolytes were stored in a desiccator until taken into the drybox.

Electrochemical Instrumentation. Electrochemical instrumentation consisted of an EG&G Princeton Applied Research (PAR) Model 173 potentiostat, PAR Model 176 current-to-voltage converter, and PAR Model 175 programmer. Positive feedback compensation of solution resistance was employed. At scan rates up to 0.5 V/s, the voltammograms were recorded with a BD 90 902/902 Kipp & Zonen XY recorder. All data at faster scan rates were acquired using a Model 4094 Nicolet digital oscilloscope that was interfaced to an IBM PC AT computer.

For scan rates less than 0.5 V/s, a large (0.70- or 0.50-cm diameter) platinum disk working electrode was used. For faster scan rates, a microelectrode (200-μm diameter) was used.[8] Between experiments these electrodes were polished with 0.05-μm alumina (Buehler) and placed in concentrated nitric acid for 5 min. A coil of platinum wire served as counter electrode. The silver reference electrode (AgRE) comprised a silver wire in contact with about 0.01 M $AgNO_3$ and 0.20 M $TBAPF_6$ in acetonitrile or 0.01 M $AgClO_4$ and 0.40 M $TBAPF_6$ in dichloromethane. Potential measurements at temperatures near ambient were also referenced to the reversible potential of ferrocene/ferrocenium as an internal standard. Unless otherwise noted, the potentials reported are the reversible voltammetric half-wave potentials which are assumed to differ negligibly from the formal potentials of the redox couples.

All electrochemical measurements were performed in a Vacuum Atmospheres drybox. The solutions typically contained ca. 0.5 mM compound and were stirred between scans using a magnetic stir bar controlled by a stirring motor located beneath the electrochemical cell. Temperature was monitored with a Trendicator digital thermometer with the thermocouple junction placed within the cell. The thermometer was calibrated at −78, 0, and 100 °C. Temperature control at temperatures below ambient was achieved by passing nitrogen gas through a glass jacket that surrounded the cell sample compartment. The temperature of the nitrogen gas was controlled by passing it through a coil of copper tubing immersed in liquid nitrogen. The cell temperature was then adjusted by controlling the nitrogen flow rate.

Digital Simulations. Simulation of cyclic voltammograms corresponding to the scheme encountered in this work was achieved by use of the standard explicit finite difference method.[9]

Table I. Reversible Potentials for Reduction of C_{60} and Metal Derivatives[a]

	E°_{i}	$E^\circ_{i^-}$	$E^\circ_{i^{2-}}$
C_{60}	−0.86	−1.44	−2.00
$(Ph_3P)_2Pt(\eta^2\text{-}C_{60})$	−1.21	−1.75	−2.23
$[(Et_3P)_2Pt]_n(\eta^2\text{-}C_{60})$			
n = 1	−1.20	−1.73	−2.27
n = 2	−1.51		
n = 3	−1.93		
n = 4	−2.31[b]		
$(Et_3P)_2Pd(\eta^2\text{-}C_{60})$	−1.18	−1.69	−2.23[b]
$(Et_3P)_2Ni(\eta^2\text{-}C_{60})$	−1.20	−1.74	−2.32

[a] V vs ferrocene/ferrocenium couple. 0.20 M $TBAPF_6$ in tetrahydrofuran. Ambient temperature. See Scheme I for definitions. The values reported are the reversible voltammetric half-wave potentials which are assumed to differ negligibly from the formal potentials of the couples. Estimated error: ±0.02 V. [b] Irreversible reaction. The value shown is the cathodic peak potential at 0.20 V/s.

Results

C_{60} Reduction. There have been several reports in the literature on the electrochemical reduction of C_{60}.[1h,2] We have been able to reproduce the reversible potentials reported for these reductions using ferrocene/ferrocenium as an internal reference. These values are reported in Table I. It should be pointed out that Dubois et al. have found that the exact values of the reduction potentials depend on both electrolyte and solvent.[2b,d,f] In this study, the solvent and electrolyte concentration were kept constant to enable

(3) (a) McCauley, J. P., Jr.; Zhu, Q.; Coustel, N.; Zhou, O.; Vaughan, G.; Idziak, S. H. J.; Fischer, J. E.; Tozer, S. W.; Groski, D. M.; Bykovetz, N.; Lin, C. L.; McGhie, A. R.; Allen, B. H.; Romanow, W. J.; Denenstein, A. M.; Smith, A. B., III *J. Am. Chem. Soc.* **1991**, *113*, 8537–8538. (b) Zhou, O.; Fischer, J. E.; Coustel, N.; Kycia, S.; Zhu, Q.; McGhie, A. R.; Romanow, W. J.; McCauley, J. P., Jr.; Smith, A. B., III; Cox, D. E. *Nature* **1991**, *351*, 462–464.

(4) Suzuki, T.; Li, Q.; Khemani, K. C.; Wudl, F.; Almarsson, Ö. *Science* **1991**, *254*, 1186–1188.

(5) (a) Koefod, R. S.; Hudgens, M. F.; Shapley, J. R. *J. Am. Chem. Soc.* **1991**, *113*, 8957–8958. (b) Koefod, R. S.; Xu, C.; Lu, W.; Shapley, J. R.; Hill, M. G.; Mann, K. R. *J. Phys. Chem.* **1992**, *96*, 2928–2930. We thank Prof. John R. Shapley for a preprint and for discussions regarding this work.

(6) (a) Fagan, P. J.; Calabrese, J. C.; Malone, B. *Science* **1991**, *252*, 1160–1161. (b) Fagan, P. J.; Calabrese, J. C.; Malone, B. In *Fullerenes*; Hammond, G. S., Kuck, V. J., Eds.; ACS Symp. Ser.; American Chemical Society: Washington DC, 1992; Chapter 12, pp 177–186. (c) Fagan, P. J.; Calabrese, J. C.; Malone, B. *J. Am. Chem. Soc.* **1991**, *113*, 9408–9409. (d) Fagan, P. J.; Calabrese, J. C.; Malone, B. *Acc. Chem. Res.* **1992**, *25*, 134–142. (e) Fagan, P. J., manuscript in preparation. (f) Chase, B.; Fagan, P. J. *J. Am. Chem. Soc.* **1992**, *114*, 2252–2256.

(7) (a) Yoshida, T.; Matsuda, T.; Otsuka, S. *Inorg. Synth.* **1990**, *28*, 98–135. (b) Schunn, R. A. *Inorg. Chem.* **1976**, *15*, 208–212.

(8) Bowyer, W. J.; Evans, D. H. *J. Electroanal. Chem.* **1988**, *240*, 227–237.

(9) Feldberg, S. W. In *Electroanalytical Chemistry. A Series of Advances*; Bard, A. J., Ed.; Marcel Dekker: New York, 1969; Vol. 3, pp 199–296.

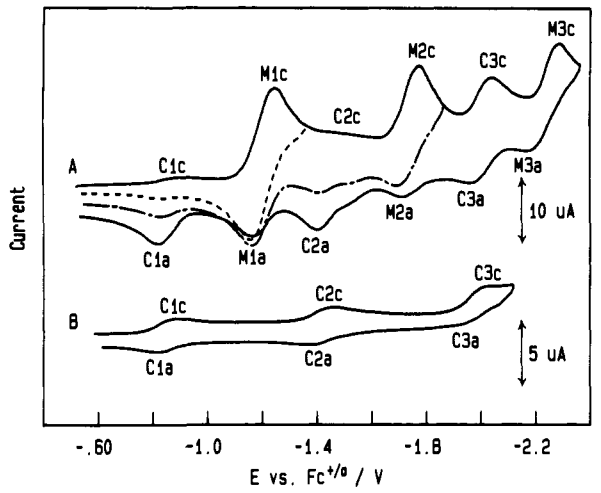

Figure 1. Cyclic voltammograms of 0.3 mM $(Ph_3P)_2Pt(\eta^2\text{-}C_{60})$ (A) and saturated C_{60} (B) (0.20 M $TBAPF_6$ in tetrahydrofuran, platinum disk working electrode, 0.20 V/s, 25 °C). Peak labeling: for example, C1c = first cathodic peak of C_{60}; M2a = anodic peak associated with the second redox process of the metal complex.

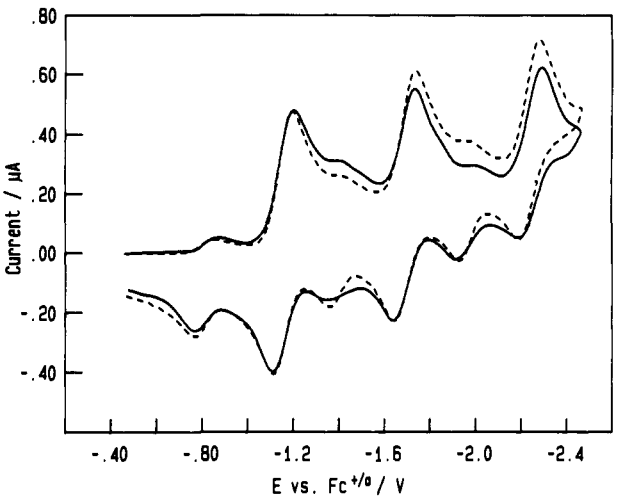

Figure 2. Solid line: Cyclic voltammogram of $(Ph_3P)_2Pt(\eta^2\text{-}C_{60})$ at 50 V/s (solid) (0.20 M $TBAPF_6$ in tetrahydrofuran, 200 µm diameter platinum disk working electrode, 25 °C). Dashed line: Digital simulation using reversible potentials given in Table I (except $E^0_{MC_{60}^{2-}}$ which is 70 mV more negative) and dissociation rate constants given in Table II. Initial concentration of C_{60} was set at 9% that of the complex. All electron transfer reactions were simulated as close-to-reversible ($k_s \geq 0.1$ cm/s, where k_s is the standard heterogeneous electron transfer rate constant).

direct comparison of results except where stated otherwise.

Reduction of $(Ph_3P)_2Pt(\eta^2\text{-}C_{60})$. Cyclic voltammograms of C_{60} and the platinum complex $(Ph_3P)_2Pt(\eta^2\text{-}C_{60})$ are shown in Figure 1. Upon reduction, the solution of this platinum complex shows an initial reduction wave (C1c; "c" denotes a cathodic peak, "a" an anodic peak) at −0.86 V attributed to ca. 8% free C_{60} in the solution. This small amount of C_{60} is probably due to some decomposition of the platinum complex caused by impurities in the electrochemical cell. This is not totally unexpected considering the complex is present in very low concentration (0.3 mM). Similar amounts of C_{60} were detected using a different solvent (CH_2Cl_2) and electrolyte (TBAP). We have not rigorously ruled out that an equilibrium exists among the complex, C_{60}, and some form of the metal fragment, P_2M, and that K_0 has a substantial value in the presence of electrolyte (see Scheme I). NMR studies (^{13}C and ^{31}P) in tetrahydrofuran alone suggest that $K_0 \leq 0.0005$ in the case of $(Ph_3P)_2Pt(\eta^2\text{-}C_{60})$.[6] The amount of complexed relative to uncomplexed C_{60} is different from sample to sample and does not vary in a well-defined way with temperature or the concentration of the platinum complex. In the simulations of the voltammograms (vide infra), the solution was treated as a mixture of complex and C_{60}, the relative concentration of the latter being adjusted to match the relative heights of the first reduction peaks due to C_{60} and the complex. It is important to note that none of the conclusions we reach in this paper depend on the actual mechanism for producing free C_{60} in solution.

As can be seen in Figure 1, there are three reduction waves (M1c, M2c, M3c) assigned to the platinum complex corresponding to formation of $(Ph_3P)_2Pt(\eta^2\text{-}C_{60})^-$, $(Ph_3P)_2Pt(\eta^2\text{-}C_{60})^{2-}$, and $(Ph_3P)_2Pt(\eta^2\text{-}C_{60})^{3-}$. Each of the reduction potentials is shifted 0.23–0.35 V to more negative potentials relative to C_{60} (see Table I). The height of these reduction peaks is consistent with successive one-electron reductions of the complex. In between these reduction events are waves which correspond to the reduction of C_{60}^- to C_{60}^{2-} (C2c) and C_{60}^{2-} to C_{60}^{3-} (C3c). Upon reversing the scan, besides the oxidation peaks (M3a, M2a, M1a) for the three platinum species $(Ph_3P)_2PtC_{60}^{3-}$, $(Ph_3P)_2PtC_{60}^{2-}$, and $(Ph_3P)_2PtC_{60}^-$, three peaks (C3a, C2a, C1a) are observed which correspond to the oxidation of C_{60}^{3-}, C_{60}^{2-}, and C_{60}^- which are now present in substantial amounts. We conclude that the anions $(Ph_3P)_2Pt\text{-}(\eta^2\text{-}C_{60})^{x-}$ (x = 1–3) are unstable with respect to dissociation of the metal fragment $(Ph_3P)_2Pt$ and formation of the anions C_{60}^-, C_{60}^{2-}, and C_{60}^{3-}, respectively. Scans reversed after the second (M2c) and third (M3c) reduction peaks qualitatively show that increasing amounts of the C_{60} anions are released as the negative charge on the complex is increased (Figure 1). As shown in Figure 2, if the scan rate was increased from 0.2 to 50 V/s, substantially less dissociation of the metal from the C_{60} anions was observed after each reduction wave. The rate of dissociation of the metal fragment is now slow relative to the scan speed.

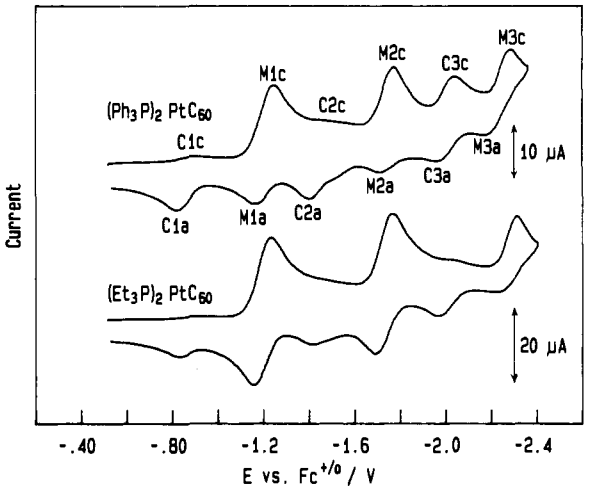

Figure 3. Comparison of cyclic voltammograms of $(Ph_3P)_2Pt(\eta^2\text{-}C_{60})$ and $(Et_3P)_2Pt(\eta^2\text{-}C_{60})$ (0.20 M $TBAPF_6$ in tetrahydrofuran, platinum disk working electrode, 0.20 V/s, ambient temperature).

Reduction of $(Et_3P)_2M(\eta^2\text{-}C_{60})$ (M = Ni, Pd, Pt). Results very similar to those for $(Ph_3P)_2Pt(\eta^2\text{-}C_{60})$ are found for all the other monosubstituted complexes $(Et_3P)_2M(\eta^2\text{-}C_{60})$ (M = Ni, Pd, Pt). Relative to platinum, a larger amount of C_{60} was initially present in solutions of the Ni and Pd complexes. Again this may arise from equilibrium metal dissociation from C_{60} and/or some initial decomposition of the complex but does not affect our conclusions. Comparison of the results for the two complexes $(Ph_3P)_2Pt(\eta^2\text{-}C_{60})$ and $(Et_3P)_2Pt(\eta^2\text{-}C_{60})$ (Figure 3) shows that the anions of the bis(triethylphosphine)platinum complex are more stable with respect to loss of C_{60} anions as judged by the smaller peaks observed for the C_{60} species. Indeed, up to four reduction waves can be observed for this complex. Figure 4 shows a comparison of the bis(triethylphosphine)nickel, -palladium, and -platinum complexes. Qualitatively, looking at the relative intensity of the reduction peaks (C2c and C3c) due to formation of C_{60}^{2-} and C_{60}^{3-} in solution, it is evident that the rate of dissociation follows the order Ni > Pd > Pt. Some broadening and distortion of the C_{60} peaks is seen for all of the complexes, suggesting that small amounts of other electroactive species are being formed.

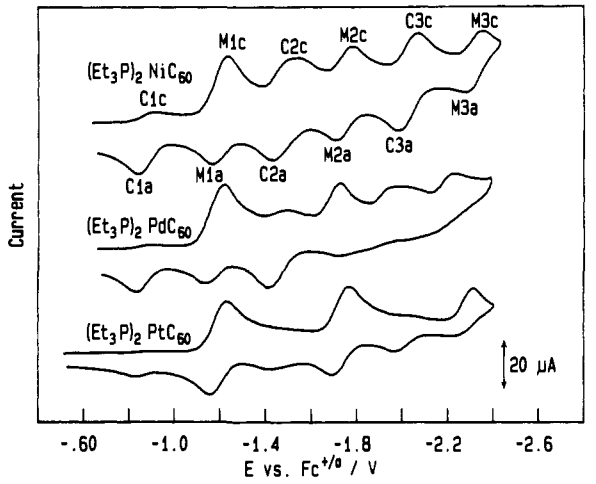

Figure 4. Comparison of cyclic voltammograms of $(Et_3P)_2M(\eta^2\text{-}C_{60})$, M = Ni, Pd, Pt (0.20 M $TBAPF_6$ in tetrahydrofuran, platinum disk working electrode, 0.20 V/s, ambient temperature).

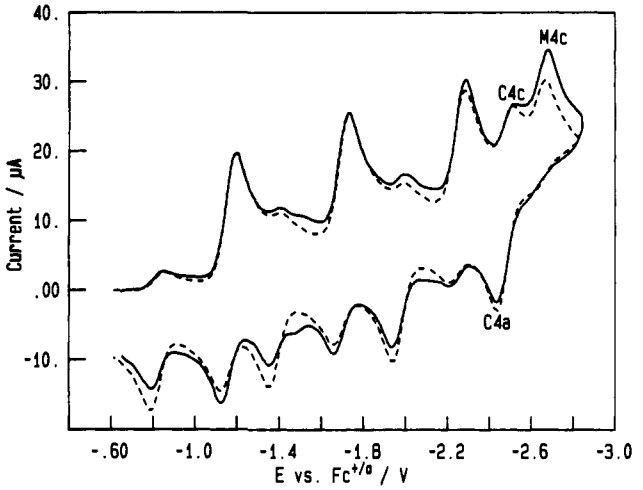

Figure 5. Solid line: Cyclic voltammogram of $(Ph_3P)_2Pt(\eta^2\text{-}C_{60})$ at −19 °C (solid) (0.20 M $TBAPF_6$ in tetrahydrofuran, platinum disk working electrode, 0.20 V/s). Dashed line: Simulation using reversible potentials given in Table I (except $E^0_{MC_{60}^{2-}}$ which is 70 mV more negative) and dissociation rate constants given in Table II. Initial concentration of C_{60} was set at 11% that of the complex. All electron transfer reactions were simulated as close-to-reversible ($k_s \geq 0.1$ cm/s, where k_s is the standard heterogeneous electron transfer rate constant).

Effect of Temperature. The rates of dissociation of the anions of the complexes are suppressed at lower temperature. Results for $(Ph_3P)_2Pt(\eta^2\text{-}C_{60})$ at −19 °C are shown in Figure 5 where the reduced magnitudes of peaks C3c and C4c reflect the smaller values of the rate constants for dissociation of $P_2MC_{60}^{2-}$ and $P_2MC_{60}^{3-}$ (vide infra) compared to room temperature. The negative potential limit is somewhat extended at low temperatures, allowing the resolution of a fourth reduction peak for C_{60} (C4c) and the complex (M4c), as well as a peak due to oxidation of C_{60}^{4-} (C4a).

Simulation of Cyclic Voltammogram Results. In order to obtain a more quantitative picture of the above results, the cyclic voltammograms of the monosubstituted metal derivatives were simulated on the basis of the extended kinetic square scheme ("fence scheme"[10]) shown in Scheme I. The decomposition of the complexes was taken into account by adjusting for an initial concentration of C_{60} in solution at the start of the simulation. The various rate constants and reduction potentials were determined by iteration until a good fit of the data was obtained. To simplify this process, good fits were obtained first for cyclic voltammograms which were run to potentials just beyond the first reduction wave

(10) Evans, D. H. *Chem. Rev.* **1990**, *90*, 739–751.

Scheme I

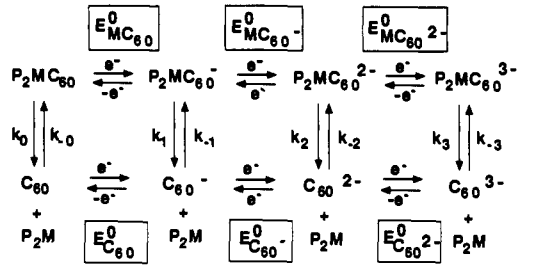

$K_0 = [P_2M][C_{60}]/[P_2MC_{60}]$ $K_1 = [P_2M][C_{60}^-]/[P_2MC_{60}^-]$

$K_2 = [P_2M][C_{60}^{2-}]/[P_2MC_{60}^{2-}]$ $K_3 = [P_2M][C_{60}^{3-}]/[P_2MC_{60}^{3-}]$

of the complex. Then the rate constant k_1 and the potentials so determined were maintained constant in simulations run to potentials beyond the second reduction wave of the metal complex. Thus, values of k_2 and $E^0_{MC_{60}^-}$ could be determined. In this manner, the simulation was extended to cover the entire cyclic voltammogram (see Figure 2). The simulations were visually compared with the experimental data, and parameters were adjusted until an acceptable fit was obtained.

As seen in Figure 2, the cyclic voltammogram for $(Ph_3P)_2Pt(\eta^2\text{-}C_{60})$ was simulated reasonably well except for a minor redox process at −1.5 V owing to an unidentified species, possibly a small amount of the disubstituted complex $[(Ph_3P)_2Pt]_2(\eta^2\text{-}C_{60})$ which is expected to be reduced at this potential (vide infra). The simulations became more difficult at more negative potentials, which in part was due to a process which removes C_{60}^{3-} from solution. Experiments with C_{60} alone indicated that C_{60}^{3-} is not stable for prolonged periods under our experimental conditions as a result of either precipitation or chemical decomposition. Inclusion of an irreversible decomposition step for C_{60}^{3-} in the simulation allows for a better fit. Also, there are numerous possible solution electron transfer (SET) reactions (e.g., eq 1) that can

$$C_{60}^{3-} + P_2MC_{60}^- \rightleftharpoons C_{60}^{2-} + P_2MC_{60}^{2-} \quad (1)$$

affect the voltammetric response. The effects of six of these SET reactions were explored but none had a significant effect on the values of the best fit parameters, i.e., less than 30% effect on the rate constants. In view of the extreme complexity of the voltammograms, the inclusion of refinements such as decomposition of C_{60}^{3-} and SET reactions did not seem warranted and they were omitted from the final simulation program.

In general, with use of these procedures the cyclic voltammograms of the monosubstituted Pt complexes were simulated quite well, with the Pd and Ni complexes being somewhat more difficult to treat particularly beyond the first reduction peak of the complexes. From extensive simulation of the cyclic voltammograms at different scan rates and temperatures, the potentials and rate constants for dissociation were obtained for the metal complexes, and are compiled in Tables I and II, respectively.

Reduction of $[(Et_3P)_2Pt]_n(C_{60})$ (n = 0–6). For the $[(Et_3P)_2Pt]_n(C_{60})$ series, we were able to evaluate the reversible potential for insertion of the first electron into the complexes for n = 0–4. The data for n = 0–4 are given in Table I. Voltammograms of solutions of the bis-complex $[(Et_3P)_2Pt]_2(C_{60})$ showed a small reduction peak for the mono-complex $(Et_3P)_2Pt(\eta^2\text{-}C_{60})$ and a major reversible process assignable to the bis-complex at −1.51 V. A sample of the tris-complex $[(Et_3P)_2Pt]_3(C_{60})$ produced a minor reversible set of peaks for the bis-complex at −1.51 V and a second major process at −1.93 V which we assign to the tris-complex. Likewise, a voltammogram of a solution of tetrasubstituted complex $[(Et_3P)_2Pt]_4(C_{60})$ showed a small peak for the tris-complex, followed by a larger peak at −2.31 V due to the tetrasubstituted complex. The hexasubstituted complex (n = 6) produced a very small peak at −2.32 V (assigned to $[(Et_3P)_2Pt]_4(C_{60})$) followed by a series of unresolved reduction processes culminating in a large, irreversible reduction peak at −3.0 V.

Table II. Rate Constants for Dissociation of the Monosubstituted C_{60} Derivatives[a]

compound	temp (°C)	k_1 (s^{-1})	k_2 (s^{-1})	k_3 (s^{-1})
$(Ph_3P)_2Pt(\eta^2\text{-}C_{60})$	25	0.006	0.94	105
	19	nd	0.43	nd
	14	nd	0.26	nd
	9	nd	0.17	nd
	4	nd	0.08	nd
	−14	*b*	*b*	1.8
	−19	*b*	*b*	0.73
	−23	*b*	*b*	0.37
$(Et_3P)_2Pt(\eta^2\text{-}C_{60})$	25	*b*	0.034	1.44
$(Et_3P)_2Pd(\eta^2\text{-}C_{60})$	25	0.29	nd	nd
	8	0.17	nd	nd
	−2	0.086	nd	nd
	−12	0.040	nd	nd
$(Et_3P)_2Ni(\eta^2\text{-}C_{60})$	21	0.95	nd	nd
	10	0.39	nd	nd
	4	0.25	nd	nd

[a] See Scheme I for definitions. 0.20 M $TBAPF_6$ in tetrahydrofuran. $k_0 \leq 0.005$ s^{-1} in all cases. Activation energies: $(Ph_3P)_2Pt(\eta^2\text{-}C_{60})$, k_2 = 19 kcal/mol, k_3 17 kcal/mol; $(Et_3P)_2Pd(\eta^2\text{-}C_{60})$, k_1 = 8 kcal/mol; $(Et_3P)_2Ni(\eta^2\text{-}C_{60})$, k_1 = 13 kcal/mol. nd: not determined. Maximum uncertainty in rate constants: ±30%. [b] Too small to be determined.

Table III. Oxidation Potentials for Metal Derivatives of C_{60} and Methyl Acrylate[a]

compound	E_{pa} Ni	E_{pa} Pd	E_{pa} Pt
$(Et_3P)_2M(\eta^2\text{-}C_2H_3CO_2CH_3)$	−0.33	+0.01	+0.15
$(Ph_3P)_2M(\eta^2\text{-}C_{60})$			+0.42
$[(Et_3P)_2M]_n(\eta^2\text{-}C_{60})$			
n = 1	+0.08	+0.20	+0.33
n = 2	−0.14[b]	−0.02[b]	+0.13
n = 3	−0.36[b]	−0.22[b]	−0.10
n = 4	−0.61[b]	−0.44[b]	−0.40
n = 5	−0.80[b]	−0.58[b]	−0.51[b]
n = 6	−0.98	−0.7[c]	−0.75

[a] V vs ferrocene/ferrocenium couple. Irreversible anodic peak potential (E_{pa}) reported at 0.20 V/s. Ambient temperature. [b] Tentative assignment based on the observation of a peak at this position in the voltammogram of a solution of hexasubstituted complex. [c] Shoulder.

Oxidation of $(R_3P)_2M(\eta^2\text{-}C_{60})$. Each of the monosubstituted complexes $(R_3P)_2M(\eta^2\text{-}C_{60})$ (R = Ph, M = Pt; R = Et, M = Ni, Pd, Pt) underwent an irreversible oxidation reaction with a peak height that was approximately two times the magnitude of the first reduction peak, suggesting an irreversible M(0) to M(II) oxidation. The ease of oxidation occurs in the order Ni > Pd > Pt (Table III). This is the same order observed for the model complexes $(Et_3P)_2M(\eta^2\text{-}CH_2{=}CHCO_2CH_3)$ (M = Ni, Pd, Pt) (Table III).

Oxidation of $[(Et_3P)_2M]_6(C_{60})$ (M = Ni, Pd, Pt). Oxidation of the hexasubstituted derivatives was investigated and, interestingly, six irreversible oxidation peaks were seen. An assignment of these oxidation processes to specific species was assisted by studies of solutions of the di-, tri-, and tetrasubstituted platinum derivatives. The disubstituted compound shows two oxidation peaks, the first assigned to oxidation of that compound and the second falling at the same potential as oxidation of the monosubstituted compound. The presence of the second peak can be due in part to some monosubstituted compound being present in solution and also possibly because oxidation of the disubstituted compound results in expulsion of an oxidized metal fragment leaving the next lower derivative to be oxidized. Similarly, the trisubstituted compound showed three oxidations with the latter two appearing at the same potential as the previously assigned oxidations of the di- and monosubstituted derivative. The peak potential assigned to the tetrasubstituted derivative is the first oxidation peak seen from a solution of that complex. The oxidation potential for the pentasubstituted compound is tentative and is based on the appearance of a peak at an intermediate potential in voltammograms of solutions of the hexasubstituted platinum derivative (Table III). The assignments of peak potentials for oxidation of the nickel and palladium derivatives were based in an analogous fashion on voltammograms of the hexasubstituted derivatives. The day-to-day reproducibility of all of these irreversible oxidation potentials was variable (as much as ±30 mV) but the trends were always reproduced: the ease of oxidation increased with the extent of substitution and, for a given substitution level, Ni > Pd > Pt.

Discussion

C_{60} Electrochemistry. As pointed out, C_{60} behaves chemically as an electron-poor species, readily binding electron-rich metal complexes.[6] Both the electrochemical[1h,2] and gas phase electron affinity[11] studies are in agreement with this. Allemand et al. have previously suggested that one can think of the pyracylene unit being present on the C_{60} surface.[2c] In retrospect, this would not be a major resonance contributor since placing double bonds in the five-membered rings of C_{60} costs energy,[12] and the bonds within the five-membered rings have been found to be much longer than those exo to the five-membered rings.[13] Analogy to these systems should be made with caution since these are planar aromatic systems whereas C_{60} is not.

From gas-phase studies, the electron affinity of C_{60} appears to be about 2.6–2.8 eV.[11] This is an extremely large number and fully consistent with the first reversible reduction potential seen in this system (−0.86 V vs. ferrocene/ferrocenium). Solution-phase redox potentials are often found to correlate linearly with gas-phase electron affinities[14] with slopes that are close to unity (d(E^0)/d(electron affinity) = 0.92 in one study).[15] The reversible potential for anthracene to its anion radical in tetrahydrofuran is −2.504 V vs ferrocene/ferrocenium, and its electron affinity is 0.57 eV. Assuming a linear relationship between E^0 and electron affinity with a slope of 0.92, the reversible potential for C_{60} should be in the range −0.45 to −0.63 V, close to the observed value of −0.86 V. Alternatively, we may take the reversible potential for tetrafluoro-1,4-benzoquinone with an electron affinity of 2.7 V, similar to C_{60}. The E^0 value for this molecule is −0.525 V vs ferrocene/ferrocenium in tetrahydrofuran, again reasonably close to the first reduction of C_{60}. Thus the magnitudes of the reversible potentials are consistent with the electron affinity data.

Electrochemistry of Metal–C_{60} Complexes. The separation between standard reduction potentials for C_{60} range from 0.4 to 0.6 V with the addition of each successive electron becoming more difficult. Values of 0.58 V ($E^0_{C_{60}} - E^0_{C_{60}^-}$) and 0.56 V ($E^0_{C_{60}^-} - E^0_{C_{60}^{2-}}$) found in the present work fall in this range. Interestingly, the monosubstituted metal complexes follow the same pattern, giving average separations of 0.53 V between the first and second reductions and 0.56 V between the second and third reductions. The similar separations between successive reversible potentials for C_{60} and the $(R_3P)_2M(\eta^2\text{-}C_{60})$ complexes coupled with the ca. −0.3 V offset of the metal complexes bring about the fortuitous and striking pattern of six sets of equally spaced voltammetric peaks in the cyclic voltammograms (for example, see Figure 1).

The simulation of the cyclic voltammograms for the monosubstituted metal derivatives was somewhat facilitated by the

(11) (a) Curl, R. F.; Smalley, R. E. *Science* **1988**, *242*, 1017–1022. (b) Yang, S. H.; Pettiette, C. L.; Conceicao, J.; Chesnovsky, O.; Smalley, R. E. *Chem. Phys. Lett.* **1987**, *139*, 233–238.

(12) Dixon, D. A.; Matsuzawa, N.; Fukunaga, T.; Tebbe, F. *J. Phys. Chem.*, submitted for publication. We thank these authors for a preprint of this work.

(13) (a) Haser, M.; Almlof, J.; Scuseria, G. E. *Chem. Phys. Lett.* **1991**, *181*, 497–500 and references therein. (b) Yannoni, C. S.; Bernier, P. P.; Bethune, D. S.; Meijer, G.; Salem, J. R. *J. Am. Chem. Soc.* **1991**, *113*, 3190–3192. (c) David, W. I. F.; Ibberson, R. M.; Matthewman, J. C.; Prassides, K.; Dennis, T. J. S.; Hare, J. P.; Kroto, H. W.; Taylor, R.; Walton, D. R. M. *Nature* **1991**, *353*, 147. (d) Liu, S.; Lu, Y. J.; Kappes, M. M.; Ibers, J. A. *Science* **1991**, *254*, 408–410. (e) Hedberg, K.; Hedberg, L.; Bethune, D. S.; Brown, C. A.; Dorn, H. C.; Johnson, R. D.; de Vries, M. *Science* **1991**, *254*, 410–412.

(14) Shalev, H.; Evans, D. H. *J. Am. Chem. Soc.* **1989**, *111*, 2667–2674 and references therein.

(15) Dewar, M. J. S.; Hashmall, J. A.; Trinajstič, N. *J. Am. Chem. Soc.* **1970**, *92*, 5555–5559.

Table IV. Thermodynamics of Dissociation of Monosubstituted Complexes as a Function of Extent of Reduction[a]

compound	$\Delta\Delta G°(0,1)$ (kcal/mol)	$\Delta\Delta G°(1,2)$ (kcal/mol)	$\Delta\Delta G°(2,3)$ (kcal/mol)
$(Ph_3P)_2Pt(\eta^2\text{-}C_{60})$	−8.1	−7.1	−5.3
$(Et_3P)_2Pt(\eta^2\text{-}C_{60})$	−7.8	−6.7	−6.2
$(Et_3P)_2Pd(\eta^2\text{-}C_{60})$	−7.4	−5.8	−5.3
$(Et_3P)_2Ni(\eta^2\text{-}C_{60})$	−7.8	−6.9	−7.4

[a] Computed from data in Table I according to eqs 6 and 7 and analogs. $\Delta\Delta G°(n-1,n) = \Delta G°(n) - \Delta G°(n-1)$.

argument that the reverse rate constants k_{-1}, k_{-2}, k_{-3} are negligibly small during the time scale of the experiment as shown by the following reasoning. First we obtain the relationship between K_0, K_1, $E^0_{C_{60}}$, and $E^0_{MC_{60}}$. One way of doing this is to write the Nernst equation for the $P_2MC_{60}/P_2MC_{60}^-$ couple:

$$E = E^0_{MC_{60}} + (RT/F)\ln\left(\frac{[P_2MC_{60}]}{[P_2MC_{60}^-]}\right) \quad (2)$$

$$= E^0_{MC_{60}} + (RT/F)\ln\left(\frac{[P_2M][C_{60}]/K_0}{[P_2M][C_{60}^-]/K_1}\right) \quad (3)$$

$$= E^0_{MC_{60}} + (RT/F)\ln(K_1/K_0) + (RT/F)\ln\left(\frac{[C_{60}]}{[C_{60}^-]}\right) \quad (4)$$

When $[C_{60}] = [C_{60}^-]$, the potential must be equal to $E^0_{C_{60}}$ so

$$E^0_{C_{60}} = E^0_{MC_{60}} + (RT/F)\ln(K_1/K_0) \quad (5)$$

$$K_1/K_0 = \exp[(F/RT)(E^0_{C_{60}} - E^0_{MC_{60}})] \quad (6)$$

$$\Delta\Delta G°(0,1) = -RT\ln(K_1/K_0) \quad (7)$$

This process can be extended to find K_2/K_1 and K_3/K_4. Unfortunately, the absolute values of the equilibrium constants are not known. Although NMR studies suggest a much smaller value, let us assume a conservative value for K_0 (i.e. k_0/k_{-0}) of ≤ 0.05 for $(Ph_3P)_2Pt(\eta^2\text{-}C_{60})$. This means $\Delta G° \geq +1.8$ kcal/mol for $P_2MC_{60} \rightleftharpoons P_2M + C_{60}$. The voltammetry shows that $P_2MC_{60}^-$ dissociates, giving C_{60}^- and P_2M. Hence it is likely that $K_1 \geq 10$. From eq 6, $K_1/K_0 = 8.2 \times 10^5$, so this corresponds to estimated limits of 1×10^{-5} to 0.05 for K_0 ($+6.8 > \Delta G°(0) > +1.8$ kcal/mol) and 10 to 4×10^4 for K_1 ($-1.4 > \Delta G°(1) > -6.3$ kcal/mol). Extending this analysis to K_2 and K_3 shows that the addition of the second and third electrons produces values of the dissociation constants which are several orders of magnitude larger. It can be seen that in general K_n is always greater than K_{n-1}, i.e. insertion of electrons weakens the Pt–C_{60} bond. Addition of two electrons is sufficient to remove any tendency of C_{60}^{2-} to bind to the P_2M fragment. From this we can conclude that k_{-1} is at least an order of magnitude less than k_1, and k_{-2} and k_{-3} are many orders of magnitude less than the k_2 and k_3. Thus we could justifiably neglect all back reactions in the simulations of the cyclic voltammograms.

The relative equilibrium constants can also be presented as $\Delta\Delta G°$ values which are listed in Table IV. The $\Delta\Delta G°$'s are the differences in the free energies of dissociation for the different redox states. For example, for $(Ph_3P)_2Pt(\eta^2\text{-}C_{60})$, $\Delta\Delta G°(0,1) = -8.1$ kcal/mol, which signifies that loss of C_{60}^- from $(Ph_3P)_2Pt(\eta^2\text{-}C_{60})^-$ is 8.1 kcal/mol more favorable than loss from the neutral complex. Just as the free energy of dissociation becomes more favorable upon successive addition of electrons, the rate of dissociation also increases. A three-point Brönsted plot of $RT\ln(k_i)$ vs $\Delta\Delta G°(0,i)$ ($i = 1$–3) for $(Ph_3P)_2Pt(\eta^2\text{-}C_{60})$ at 25 °C produces the expected linear relationship between the logarithm of the forward rate constant and the driving force for loss of the metal fragment (slope = −0.46). Extrapolation of this plot gives a predicted value for k_0 of the order of 10^{-5} s^{-1} which is fully consistent with our inability to detect any dissociation of the neutral complexes on the voltammetric time scale (Table II).

We have also determined a number of the rate constants as a function of temperature, yielding activation energies for the dissociation of the metal fragment from the C_{60} core (Table II). There are two possible mechanisms for metal dissociation. One simply involves a first-order dissociation of the metal fragment, and the second involves a solvent-assisted pathway whereby the solvent first coordinates to the metal which then dissociates from C_{60}. We believe the latter is unlikely for steric reasons, especially in the case of $(Ph_3P)_2Pt(\eta^2\text{-}C_{60})$ where the platinum metal is completely surrounded by the large triphenylphosphine ligands and the C_{60} ligand. Direct dissociation of $(Ph_3P)_2Pt$ is reasonable since two-coordinate $(R_3P)_2Pt$ metal fragments are frequently proposed as reaction intermediates, and in fact can be isolated in the case of sterically hindered phosphines.[7a,16] We conclude that the activation energies are governed mainly by the metal–C_{60} anion bond strengths.

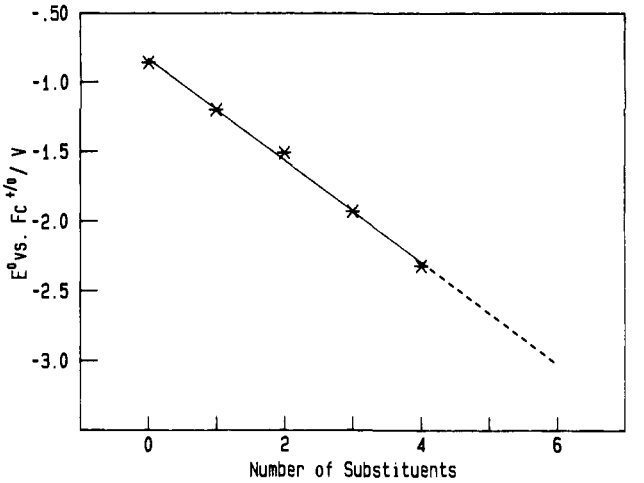

Figure 6. Reversible potentials for the first reduction step of $[(Et_3P)_2Pt]_n(C_{60})$ vs n at ambient temperature. Extrapolation shows expected potentials for $n = 5$ and 6.

The monosubstituted derivatives $(Et_3P)_2M(\eta^2\text{-}C_{60})$ (M = Ni, Pd, Pt) are 0.34 V harder to reduce than C_{60} itself. The reduction processes for all of the metal complexes are concluded to be C_{60}-based with the observed shifts arising from perturbations in electron affinity brought about by binding the metal to the C_{60} core. In support of the notion that the reductions are C_{60}-based rather than metal-based is the observation that reduction of the complexes $(Et_3P)_2M(\eta^2\text{-}CH_2{=}CHCO_2CH_3)$ does not occur anywhere in the range of potentials encompassing the metal–C_{60} reduction processes. Koefod et al. have reached a similar conclusion for the complex $(indenyl)(CO)Ir(\eta^2\text{-}C_{60})$.[5b]

Variation of C_{60} Electron Affinity with Degree of Metal Substitution. A remarkably linear relationship exists (Figure 6) between the observed reversible potentials and the degree of substitution in the series $[(Et_3P)_2Pt]_n(C_{60})$ ($n = 0$–4) with the addition of each metal fragment producing a negative shift of −0.36 V (8.3 kcal/mol) in the reduction potentials. Linear progression of potentials with sequential addition of substituents has been found in a few cases for both inorganic and organic systems.[17] Extrapolation to $n = 5$ and 6 suggests that the reversible potentials for addition of the first electron to these complexes would be near −2.7 and −3.0 V, respectively. Peaks or shoulders appeared in these potential regions in voltammograms of the hexakis-complex.

Effect of Metal Substitution. We propose the addition of a metal has several possible effects on C_{60} electronic structure. A major effect is to remove one double bond from conjugation with the remaining 29 double bonds because of metal backbonding. From X-ray results,[6] the bonding parameters are much closer to a metallocyclopropane resonance structure description (lengthening the carbon–carbon bond attached to platinum to 1.50 Å[6]). Raman

(16) (a) Paonessa, R. S.; Prignano, A. L.; Trogler, W. C. *Organometallics* **1985**, *4*, 647–657. (b) Paonessa, R. S.; Trogler, W. C. *Organometallics* **1982**, *1*, 768–770.

(17) Duff, C. M.; Heath, G. A. *Inorg. Chem.* **1991**, *30*, 2528–2535 and references therein.

studies also indicate d-backbonding from the metal to C_{60}.[6f] Removal of a double bond from conjugation in any polyene system is expected to raise the energy of the lowest unoccupied orbital, or in other words decrease the electron affinity of the molecule. Another possible effect is to "leak" some d-orbital backbonding electron density into the π^* orbitals of the remaining double bonds on the cluster. However, the extent of this latter effect is probably small. Otherwise, it is hard to explain the observation that the monosubstituted Ni, Pd, and Pt complexes $(Et_3P)_2M(\eta^2\text{-}C_{60})$ are reduced at *exactly the same potential* despite the fact that the three different metals are expected to backbond to different extents. Donation of electrons from the metal via backbonding is thus a relatively localized effect on the sphere. Upon addition of a radical to C_{60}, there is evidence that the unpaired spin does not wander far from the initial point of attack and is not delocalized over the entire sphere.[18] Thus one might not expect metal backbonding electron density to extend too far beyond the site of metal binding.

If metal backbonding is strong, one C_{60} carbon–carbon double bond is removed from conjugation. The remaining π system of 29 conjugated double bonds in part determines the electron affinity of the molecule. An estimate of how much the removal of a single double bond contributes to the decrease in electron affinity can be obtained by comparison to the compound $t\text{-}BuC_{60}H$,[19] in which the redox potential is shifted −0.15 V relative to C_{60} (cf. Ph_2CC_{60} which shifts −0.11 V[4]). The additional ca. −0.1 V shift observed in the metal derivatives relative to these organic derivatives can be attributed to a higher inductive donation of electron density into the C_{60} σ bond framework, which serves to lower the electron affinity further. As more metals are added, the electron affinity drops with coordination of subsequent electron rich metals becoming less favorable. There is evidence that the metal fragments begin to equilibrate on and off the C_{60} framework more readily in the hexasubstituted derivatives $[(Et_3P)_2M]_6C_{60}$ (M = Ni, Pd, Pt) which allows the T_h symmetry structure to be achieved in these complexes.[6d,e]

In the case of weak backbonding, some residual conjugation across the metal-coordinated C–C double bond is probable, and these types of complexes will not perturb the electron affinity of the C_{60} cluster as greatly. The metal complex (indenyl)(CO)$Ir(\eta^2\text{-}C_{60})$ may fall into this category as this has been reported by Koefod et al. to be only 0.080 V harder to reduce than C_{60}.[5b] From preliminary results, a nickel complex with less electron-donating phosphite ligands $[(o\text{-}CH_3C_6H_4O)_3P]_2Ni(\eta^2\text{-}C_{60})$ has been found to be only 0.28 V harder to reduce than C_{60}.

The decreased electron affinity of C_{60} upon binding of a metal explains why the monosubstituted complex can be formed selectively in reaction with the low-valent metal reagents. The tendency of a second metal to add is significantly reduced, and even if some disubstituted metal complex does form, there is a substantial driving force for the disubstituted derivative to react with free C_{60} in solution and form the monosubstituted derivative.

Upon reduction the complexes become unstable and the $(R_3P)_2M$ fragments are released from the C_{60} anions. The rate of this release increases with the degree of reduction, i.e. $(Et_3P)_2M(\eta^2\text{-}C_{60})^{3-} > (Et_3P)_2M(\eta^2\text{-}C_{60})^{2-} > (Et_3P)_2M(\eta^2\text{-}C_{60})^{-}$. Reducing these complexes adds additional electron density into the lowest energy π^* orbital of the cluster which is derived from the π^* orbitals of the 29 remaining double bonds with perhaps an added component of metal–C_{60} antibonding character. We propose addition of electrons to the complex drives the metals off since the metals cannot backbond as effectively into the π^* orbitals of the C_{60} anions which contain added electron density. In comparing metal loss in $(Et_3P)_2PtC_{60}^{-}$ to that in $(Ph_3P)_2PtC_{60}^{-}$, it is found that the rate of loss of the $(Ph_3P)_2M$ group is greater. The $(Ph_3P)_2Pt$ group is bulkier than $(Et_3P)_2Pt$, and also less electron-rich. Both effects should weaken the $(Ph_3P)_2Pt$-to-C_{60} bonding relative to $(Et_3P)_2Pt$.

Although the reduction of the metal complexes is independent of the metal, this is not the case for the first irreversible oxidations. For ease of oxidation, these complexes follow the order $(Et_3P)_2Ni(\eta^2\text{-}C_{60}) > (Et_3P)_2Pd(\eta^2\text{-}C_{60}) > (Et_3P)_2Pt(\eta^2\text{-}C_{60})$ (Table III). This is the same oxidation facility order observed for the complexes $(Et_3P)_2M(\eta^2\text{-}CH_2{=}CHCO_2CH_3)$ (M = Ni > Pd > Pt) (Table III). This suggests the oxidation events in these complexes are metal based. This would be expected since C_{60} itself is difficult to oxidize.[2]

Conclusion

In summary, we have shown that the electron affinity of C_{60} decreases upon binding of metals. This should be a general effect for this molecule, since any addition chemistry will decrease the number of pathways for conjugation of the carbon–carbon double bonds. The fact that the electron affinity of C_{60} can be tuned by simply adjusting the number of metals on the C_{60} core suggests that the metal groups might be used as temporary protecting groups to modify the reactivity of C_{60} and perhaps make it more controllable with regard to other addition reactions. We are pursuing this line of research.

Acknowledgment. We thank Mr. Ronald J. Davis and Mr. Ed Delawski of Du Pont for technical assistance. We also thank Professor John Shapley of the University of Illinois for helpful discussions regarding their results for (indenyl)(CO)$Ir(\eta^2\text{-}C_{60})$ and a preprint of this work. This research was supported in part by the National Science Foundation (Grant CHE9100281).

(18) (a) Krusic, P. J.; Wasserman, E.; Parkinson, B. A.; Malone, B.; Holler, E. R., Jr.; Keizer, P. N.; Morton, J. R.; Preston, K. F. *J. Am. Chem. Soc.* **1991**, *113*, 6274–6275. (b) Krusic, P. J.; Wasserman, E.; Keizer, P. N.; Morton, J. R.; Preston, K. F. *Science* **1991**, *254*, 1183–1185. (c) Krusic, P. J., personal communication.

(19) Fagan, P. J.; Krusic, P. J.; Evans, D. H.; Lerke, S. A.; Johnston, E. Submitted for publication.